



# Impact of variable fluid properties on forced convection of Fe<sub>3</sub>O<sub>4</sub>/CNT/water hybrid nanofluid in a double-pipe mini-channel heat exchanger

Amin Shahsavari<sup>1</sup> · Ali Godini<sup>1</sup> · Pouyan Talebizadeh Sardari<sup>2</sup> · Davood Toghraie<sup>3</sup> · Hamzeh Salehipour<sup>4</sup>

Received: 8 December 2018 / Accepted: 26 December 2018 / Published online: 9 January 2019  
© Akadémiai Kiadó, Budapest, Hungary 2019

## Abstract

The objective of this study is to assess the hydrothermal performance of a non-Newtonian hybrid nanofluid with temperature-dependent thermal conductivity and viscosity compared with a Newtonian hybrid nanofluid with constant thermophysical properties. A counter-current double-pipe mini-channel heat exchanger is studied to analyze the effects of the hybrid nanofluid. The nanofluid is employed as the coolant in the tube side, while the hot water flows in the annulus side. Two different nanoparticles including tetramethylammonium hydroxide-coated Fe<sub>3</sub>O<sub>4</sub> (magnetite) nanoparticles and gum arabic-coated carbon nanotubes are used to prepare the water-based hybrid nanofluid. The results demonstrated that the non-Newtonian hybrid nanofluid always has a higher heat transfer rate, overall heat transfer coefficient, and effectiveness than those of the Newtonian hybrid nanofluid, while the opposite is true for the pressure drop, pumping power, and performance evaluation criterion. Supposing that the Fe<sub>3</sub>O<sub>4</sub>-carbon nanotube/water hybrid nanofluid is a Newtonian fluid with constant thermal conductivity and viscosity, there leads to large error in the computation of pressure drop (1.5–9.71%), pumping power (1.5–9.71%), and performance evaluation criterion (18.24–19.60%), whereas the errors in the computation of heat transfer rate, overall heat transfer coefficient, and effectiveness are not considerable (less than 2.91%).

**Keywords** Non-Newtonian hybrid nanofluid · Double-pipe heat exchanger · Magnetite · Carbon nanotube · Convective heat transfer

## List of symbols

$A$	Internal tube surface area (m <sup>2</sup> )
$C_{\min}$	Minimum heat capacity rate (W K <sup>-1</sup> )
$c_p$	Specific heat capacity (J kg <sup>-1</sup> K <sup>-1</sup> )
$D_h$	Hydraulic diameter (m)
$f$	Friction factor
$h$	Convective heat transfer coefficient (W m <sup>-2</sup> K <sup>-1</sup> )
$k$	Thermal conductivity (W m <sup>-1</sup> K <sup>-1</sup> )
$L$	Length (m)

$\dot{m}$	Mass flow rate (kg s <sup>-1</sup> )
$Nu$	Nusselt number
$PEC$	Performance evaluation criterion
$p$	Pressure (Pa)
$\dot{Q}$	Heat transfer rate (W)
$Re$	Reynolds number
$r_i$	Inlet radius (m)
$r_o$	Outlet radius (m)
$T$	Temperature (K)
$\Delta T_{LMTD}$	Logarithmic mean temperature difference (K)
$U$	Overall heat transfer coefficient (W m <sup>-2</sup> K <sup>-1</sup> )
$u_{in}$	Inlet velocity (m s <sup>-1</sup> )
$V$	Velocity (m s <sup>-1</sup> )
$\dot{V}$	Volumetric flow rate (m <sup>3</sup> s <sup>-1</sup> )
$\dot{W}$	Pumping power (W)

✉ Davood Toghraie  
toghraee@iaukhsh.ac.ir

- <sup>1</sup> Department of Mechanical Engineering, Kermanshah University of Technology, Kermanshah, Iran
- <sup>2</sup> Fluids and Thermal Engineering Research Group, Faculty of Engineering, The University of Nottingham, University Park, Nottingham, UK
- <sup>3</sup> Department of Mechanical Engineering, Khomeinishahr Branch, Islamic Azad University, Isfahan, Iran
- <sup>4</sup> Department of Mechanical Engineering, Ilam University, Ilam 69315-516, Iran

## Greek symbols

$\varepsilon$	Heat exchanger effectiveness
$\mu$	Dynamic viscosity (Pa s)
$\rho$	Density (kg m <sup>-3</sup> )
$\varphi$	Volume concentration of nanoparticles (%)

## Subscripts

CNT	Carbon nanotube
i	Inlet
M	Magnetite
N	Newtonian
NN	Non-Newtonian
nf	Nanofluid
o	Outlet
s	Wall
w	Water

## Introduction

Double-pipe heat exchangers have been widely employed in various applications to exchange the heat between two fluids called as heat transfer fluids [1]. They are an essential part of almost all the industries, including the oil and gas industry, power generation, refrigeration, and nuclear power. Due to the great importance of heat exchangers, improving their efficiency is a very important issue. So far, several methods have been proposed in the literature to enhance the heat exchanger performance such as using various fins and turbulators. However, these modifications offer several disadvantages like increase in pressure drop, weight and volume of heat exchangers that limit their usage.

Over the past decade, scientists and researchers around the world have revealed that the heat exchanger performance can be considerably enhanced by improving the thermal conductivity of working fluids [2]. This goal can be achieved through the use of nanofluids, which are prepared by suspending nanoparticles with sizes typically of 1–100 nm in conventional heat transfer fluids such as water, oil, and ethylene glycol [3]. This term was first suggested by Choi [4] in 1995, and it has since gained in popularity [5].

A great number of experimental and numerical works have been performed on the various aspects of different nanofluids performance in double-pipe heat exchangers. Maddah et al. [6] experimentally evaluated the effects of  $\text{Al}_2\text{O}_3$ -water nanofluid on the performance of a horizontal double-pipe heat exchanger under turbulent flow regime and showed 52% and 12% enhancement in the friction factor and heat transfer rate, respectively. Mousavi et al. [7] numerically studied the effect of a variable magnetic field on the hydrothermal characteristics of  $\text{Fe}_3\text{O}_4$ -water nanofluid flowing through a sinusoidal double-pipe heat exchanger and reported the enhancement of Nusselt number in the presence of magnetic field. Saeedan et al. [8] numerically examined the effect of Cu-water, CuO-water and carbon nanotube (CNT)-water nanofluids on the performance of a finned-type heat exchanger. They found that

both the Nusselt number and pressure drop intensify with increasing nanoparticle concentration. Sarafraz et al. [9] experimentally studied the use of CNT-water nanofluid inside a double-pipe heat exchanger. They assessed the impact of different effective parameters on the convective heat transfer coefficient in laminar and turbulent flow regimes and found that the proposed nanofluid can enhance the heat transfer by almost 44% compared with the pure water. Kumar et al. [10] experimentally surveyed the effect of  $\text{Fe}_3\text{O}_4$ -water nanofluid on the performance of a double-pipe heat exchanger with a longitudinal fin with return bend under turbulent flow regime. They showed the enhancement of Nusselt number with increasing Reynolds number and nanoparticle concentration. Hussein [11] experimentally examined the flow of aluminum nitride-ethylene glycol nanofluid through a double-pipe heat exchanger and showed the increase in Nusselt number with increasing flow rate and volume concentration of nanofluid. Shirvan et al. [12] studied the influence of Reynolds number and nanoparticle concentration on the performance of  $\text{Al}_2\text{O}_3$ -water nanofluid inside a double-pipe heat exchanger and showed the enhancement of Nusselt number with increasing Reynolds number and decreasing nanoparticle concentration.

To enhance the rate of heat transfer, hybrid nanofluids have attracted lots of attention using a combination of different nanoparticles in the nanofluids in order to take the advantage of them. Esfe et al. [13] experimentally studied the thermal conductivity of ethylene glycol-based hybrid nanofluid containing ZnO-CNT nanoparticles. They showed the improvement of thermal conductivity using ZnO and CNT nanoparticles compared with the base fluid and developed a new correlation for the calculation of thermal conductivity based on the experimental data using an artificial neural network (ANN).

Carbon nanotubes present an outstanding mechanical, electrical, thermal, and chemical property. For example, a single nanotube is 100 times stronger than steel. It is one of the best field emission emitters, it can maintain high current density, and it has a thermal conductivity comparable to that of diamond [14]. The combination of  $\text{Fe}_3\text{O}_4$  and CNT nanoparticles is widely used as a promising hybrid nanofluid which combines the great thermal conductivity material of CNT and high magnetic material of  $\text{Fe}_3\text{O}_4$ . Baby and Sundara [15] studied the effects of nanoparticles concentration on the thermal conductivity of  $\text{Fe}_3\text{O}_4$ /CNT/water hybrid nanofluid and reported 6.5–10% improvement in the thermal conductivity of nanofluid in the temperature range of 30–50 °C compared with the base fluid. Felicia and Philip [16] investigated an oil-based  $\text{Fe}_3\text{O}_4$ /CNT hybrid nanofluid in the presence of a magnetic field and showed the enhancement of viscosity with increasing magnetic field intensity. Sundar et al. [17] experimentally

assessed the hydrothermal characteristics of Fe<sub>3</sub>O<sub>4</sub>/CNT/water hybrid nanofluid in a circular tube and presented 14.8% improvement in the Nusselt number using nanofluid with concentration of 0.3% at Reynolds number of 3000. Shahsavari et al. [18] studied the use of Fe<sub>3</sub>O<sub>4</sub>/CNT/water hybrid nanofluid in a heated tube in the presence of both constant and alternating magnetic fields. They showed higher improvement of heat transfer using a constant magnetic field compared with an alternating one. Harandi et al. [19] conducted experiments to determine the thermal conductivity of Fe<sub>3</sub>O<sub>4</sub>/CNT/EG hybrid nanofluid at different temperatures and found the improvement of thermal conductivity with the increase in temperature and nanoparticle concentration.

In most of the previous research works on the performance of heat exchangers containing various nanofluids, the thermophysical properties of the nanofluid have been assumed as constant and the nanofluid itself has been considered as Newtonian [20], while various studies have shown that the thermophysical properties of nanofluids are a function of temperature and that the majority of nanofluids exhibit a non-Newtonian behavior [21]. The aim of this research is to see whether a significant difference is observed in the performance parameters of a heat exchanger (i.e., pumping power, effectiveness, and performance evaluation criterion) by assuming constant properties and a Newtonian nature for nanofluids. It also seeks to find out: Under what conditions the assumptions of constant properties and Newtonian nature of nanofluid can be used in the analysis of heat exchangers? This is done by comparing the performance parameters of a counter-current double-pipe heat exchanger containing Newtonian Fe<sub>3</sub>O<sub>4</sub>/CNT/water nanofluid of constant properties with the performance parameters of a heat exchanger containing the non-Newtonian Fe<sub>3</sub>O<sub>4</sub>/CNT/water hybrid nanofluid with temperature-dependent thermal conductivity and viscosity, at different Reynolds numbers and concentrations.

## Physical properties of nanofluid

This investigation is conducted on a hybrid nanofluid consisting of tetramethylammonium hydroxide (TMAH)-coated magnetite nanoparticles and gum arabic (GA)-coated CNTs. It was prepared by mixing different volume ratios of Fe<sub>3</sub>O<sub>4</sub>-water nanofluid and CNT-water nanofluid, followed by 5-min sonication [22]. The detailed description of the preparation method can be found in Ref. [23]. The magnetite and CNT nanoparticles are attached physically because of interaction between the molecules of TMAH and GA.

After careful preparation and characterization, some experiments were performed to evaluate the

thermophysical properties of the hybrid nanofluid. The hybrid nanofluid shows the non-Newtonian shear-thinning behavior since there is a sharp decrease in the viscosity of nanofluid with the increase in shear rate at lower shear rates, and the viscosity becomes gradually constant at higher shear rates. The shear-thinning region is up to 70 s<sup>-1</sup>; for higher shear rates, the viscosity tends to follow the Newtonian pattern. Additionally, the viscosity of the hybrid nanofluid enhances with the increase in volume concentration of nanoparticles, while it reduces with increasing temperature. However, the thermal conductivity increases with temperature and volume concentration.

Based on the data obtained from experiments, the ANN was used to find a correlation between the thermal conductivity and temperature and volume concentration of Fe<sub>3</sub>O<sub>4</sub> and CNT nanoparticles [24]. For the viscosity, a correlation is developed as a function of temperature, shear rate, and volume concentrations of Fe<sub>3</sub>O<sub>4</sub> and CNT nanoparticles [24]. The acquired neural network models illustrate a good accuracy to predict the thermal conductivity and viscosity according to Fig. 1. The thermal conductivity model predicts the outputs with mean square error (MSE) and coefficient of determination (*R*<sup>2</sup>) values of about 1.59 × 10<sup>-5</sup> and 0.999, respectively, based on the test data. Meanwhile, MSE and *R*<sup>2</sup> values for the viscosity model are, respectively, 3.34 × 10<sup>-10</sup> and 0.999 for the test data.

The viscosity and thermal conductivity of the considered Newtonian hybrid nanofluid are reported in Table 1. The considered viscosity for the Newtonian nanofluid is equal to the viscosity of the non-Newtonian nanofluid at the same concentration of CNT and magnetite nanoparticles at shear rates higher than 70 s<sup>-1</sup>. Also, the considered thermal conductivity for the Newtonian nanofluid samples is the same as the thermal conductivity of the non-Newtonian nanofluid at the inlet temperature of nanofluid.

Moreover, the nanofluid bulk density ( $\rho_{nf}$ ) and specific heat ( $c_{p,nf}$ ) are computed as [25]:

$$\rho_{nf} = \varphi_M \rho_M + \varphi_{CNT} \rho_{CNT} + (1 - \varphi_M - \varphi_{CNT}) \rho_w \quad (1)$$

$$c_{p,nf} = \varphi_M c_{p,M} + \varphi_{CNT} c_{p,CNT} + (1 - \varphi_M - \varphi_{CNT}) c_{p,w} \quad (2)$$

where  $\varphi$  is the volume concentration of nanoparticles and, subscripts M, CNT, and w refer to magnetite, CNT, and water, respectively.

## Geometry and boundary conditions

The present investigation is conducted in a double-pipe counter-current mini-channel heat exchanger with the length of 1 m, inner diameter of 1 mm, and outer diameter

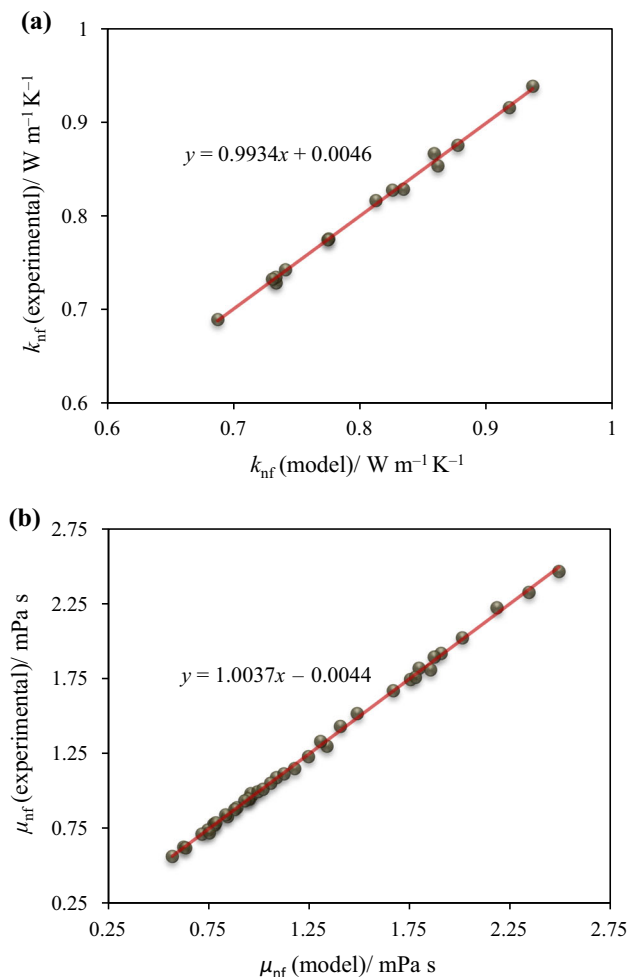


**Fig. 1** Results obtained from the developed models in comparison with the experimental data: **a** thermal conductivity and **b** viscosity [24]

of 2 mm. The thickness of the inner tube’s wall is neglected. Figure 2 illustrates the schematic of the geometry including the flow directions of both hot water and cold nanofluid. Due to the axisymmetric nature of the problem, only half of the geometry is considered as the computational 2-D domain.

### Mathematical modeling

Due to the small size of nanoparticles, the nanofluids can thus be approximately evaluated as a pure fluid considering no velocity slip and local thermal equilibrium between the base fluid and nanoparticles. The governing equations for laminar, steady-state forced convection flow of the studied nanofluid are given as follows:

Continuity:

$$\nabla \cdot (\rho_{nf} \mathbf{V}) = 0 \tag{3}$$

Momentum:

$$\nabla \cdot (\rho_{nf} \mathbf{V} \mathbf{V}) = -\nabla p + \nabla \cdot (\mu_{nf} \nabla \mathbf{V}) \tag{4}$$

Energy:

$$\nabla \cdot (\rho_{nf} c_{p,nf} T) = \nabla \cdot (k_{nf} \nabla T) \tag{5}$$

where  $\mathbf{V}$  is the velocity,  $p$  is the pressure, and  $T$  is the temperature.

For the outer wall, adiabatic boundary condition is used. Uniform velocity and uniform temperature are also considered at both tube and annulus entrances, while zero relative pressure is utilized at the outlets. Additionally, the no-slip condition is employed on the inner and outer walls.

Mathematically, all the boundary conditions are represented as follows:

Flow inlet:

$$\vec{u} = \vec{u}_0; \quad T = T_0 \tag{6}$$

Flow outlet:

$$p = p_0 \tag{7}$$

At the outer wall:

$$\vec{u} = 0; \quad \frac{\partial T}{\partial n} = 0 \tag{8}$$

At the inner wall:

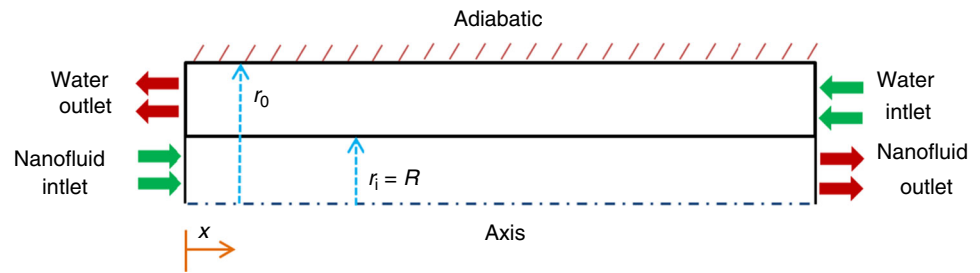
$$\vec{u} = 0 \tag{9}$$

Reynolds number for the flow of nanofluid ( $Re_{nf}$ ) and water ( $Re_w$ ) through the tube side and annulus side, respectively, can be calculated as:

**Table 1** Characteristics of the studied Newtonian nanofluid samples

	$\varphi_{CNT}/\% = 0.1\%$					$\varphi_{CNT}/\% = 1.35\%$				
	$\varphi_M/\%$					$\varphi_M/\%$				
	0.1	0.3	0.5	0.7	0.9	0.1	0.3	0.5	0.7	0.9
$\mu_{nf} \times 10^4 / \text{kg ms}^{-1}$	8.15	9.48	11.08	12.81	14.48	11.33	13.03	14.61	15.95	17.01
$k_{nf} / \text{W mK}^{-1}$	0.691	0.725	0.739	0.759	0.794	0.703	0.759	0.772	0.866	0.902

**Fig. 2** The mini-channel heat exchanger under study



$$Re_{nf} = \frac{\rho_{nf} u_{in,nf} D_{h,nf}}{\mu_{nf}} \tag{10}$$

$$Re_w = \frac{\rho_w u_{in,w} D_{h,w}}{\mu_w} \tag{11}$$

where  $D_{h,nf}$  is the hydraulic diameter of the inner tube ( $= 2r_i$ ),  $D_{h,w}$  is the hydraulic diameter of the annulus ( $= 2(r_o - r_i)$ ),  $u_{in,nf}$  is the inlet velocity of the nanofluid, and  $u_{in,w}$  is the inlet velocity of the water. In addition,  $r_i$  and  $r_o$  are the inlet radius and outlet radius of the heat exchanger, respectively.

Considering the facts that the outer wall of the heat exchanger is adiabatic and the problem under consideration is steady state, the rate of heat transfer to the nanofluid from the hot water is equal to that of the hot water according to the conservation of energy ( $\dot{Q}_{nf} = \dot{Q}_w = \dot{Q}$ ) which are obtained as [26]:

$$\dot{Q}_{nf} = \dot{m}_{nf} c_{p,nf} (T_{out} - T_{in})_{nf} \tag{12}$$

$$\dot{Q}_w = \dot{m}_w c_{p,w} (T_{in} - T_{out})_w \tag{13}$$

where  $\dot{m}_{nf}$  and  $\dot{m}_w$  are mass flow rate of the cold nanofluid and the hot water, respectively.

The overall heat transfer coefficient is given as [26]:

$$U = \frac{\dot{Q}}{A \Delta T_{LMTD}} \tag{14}$$

where  $A$  is the internal tube area, and  $\Delta T_{LMTD}$  is the logarithmic mean temperature difference computed as [26]:

$$\Delta T_{LMTD} = \frac{\Delta T_2 - \Delta T_1}{\ln(\Delta T_2 / \Delta T_1)} \tag{15}$$

where  $\Delta T_1 = T_{in,w} - T_{out,nf}$  and  $\Delta T_2 = T_{out,w} - T_{in,nf}$ . One way of measuring the performance of a heat exchanger is to compute its effectiveness. The heat exchanger effectiveness is the ratio of the actual heat transfer rate to the maximum possible one given as [26]:

$$\varepsilon = \frac{\dot{Q}}{\dot{Q}_{max}} = \frac{\dot{Q}}{C_{min} (T_{in,w} - T_{in,nf})} \tag{16}$$

where  $C_{min}$  represents the minimum heat capacity rate given as [26]:

$$C_{min} = \min[C_w, C_{nf}] \tag{17}$$

Here,  $C_w$  and  $C_{nf}$  are, respectively, heat capacity rates of the water and the nanofluid defined as [26]:

$$C_w = \dot{m}_w c_{p,w} \tag{18}$$

$$C_{nf} = \dot{m}_{nf} c_{p,nf} \tag{19}$$

The minimum heat capacity rate is obtained for the nanofluid, and hence, the effectiveness is calculated as [26]:

$$\varepsilon = \frac{T_{out,nf} - T_{in,nf}}{T_{in,w} - T_{in,nf}} \tag{20}$$

The rate of energy consumption required to pump the nanofluid into the heat exchanger is given as [26]:

$$\dot{W} = \dot{V} \Delta p \tag{21}$$

where  $\dot{V}$  is the volumetric flow rate, and  $\Delta p$  is the pressure drop of nanofluid obtained as [20]:

$$\Delta p = \frac{\rho_{nf} f L u_{in,nf}^2}{2 D_{h,nf}} \tag{22}$$

where  $L$  is the length of heat exchanger and  $f$  is the friction factor defined as  $f = \frac{64}{Re_{nf}}$  [20].

The Nusselt number of nanofluid can be computed through the following equation:

$$Nu = \frac{h D_{h,nf}}{k_{nf}} = \frac{\dot{Q}}{\pi L k_{nf} (T_s - T_{b,nf})} \tag{23}$$

where  $h$  is the convective heat transfer coefficient of the nanofluid,  $T_s$  is the wall temperature, and  $T_{b,nf}$  is the bulk temperature of the nanofluid.

The performance evaluation criterion ( $PEC$ ) is a flow criterion which examines the Nusselt number enhancement of nanofluid compared to the base fluid at equal pumping power [27]:

$$PEC = \frac{(Nu/Nu_{bf})}{(f/f_{bf})^{1/3}} \tag{24}$$

## Numerical method and validation

Finite volume method is used to solve the governing equations employing the SIMPLE method for pressure and velocity coupling. The second-order upwind method is used to discretize the convective and diffusion terms using the finite volume method. The convergence criteria are also set to  $10^{-6}$ . As shown in Fig. 3, a structured quad-based mesh was used throughout the domain with a more grid density near the wall. The grid independence study was carried out by considering the numerical results of six different grid resolutions. The results of this investigation are summarized in Table 2. It should be noted that the grid resolution was reported as number of longitudinal nodes  $\times$  number of radial nodes in central tube  $\times$  number of radial nodes in annulus. So, by comparing the results, the grid with resolution of  $1000 \times 35 \times 35$  was chosen. To verify the present numerical procedure, the results are compared with the experimental data of Duangthongsuk and Wongwises [28] for  $\text{TiO}_2$ -water nanofluid in a double-pipe heat exchanger shown in Fig. 4. Good agreement between the present results and Ref. [28] is found with the maximum error of 5%.

## Results and discussion

In this research, the influences of the shear rate and temperature-dependent viscosity and the temperature-dependent thermal conductivity on the hydrothermal characteristics of  $\text{Fe}_3\text{O}_4/\text{CNT}/\text{water}$  hybrid nanofluid flowing inside a double-pipe heat exchanger are evaluated and compared with those obtained by regarding the hybrid nanofluid as a Newtonian fluid with constant thermal conductivity and viscosity. The simulations are conducted at magnetite concentration range of 0.1–0.9%, CNT concentration range of 0–1.35%, Reynolds number range of 500–2000 for the tube side, and constant Reynolds number of 1000 for the annulus side. The inlet temperature of the nanofluid and water is considered as 298 K and 308 K, respectively. Note that the results of the non-Newtonian

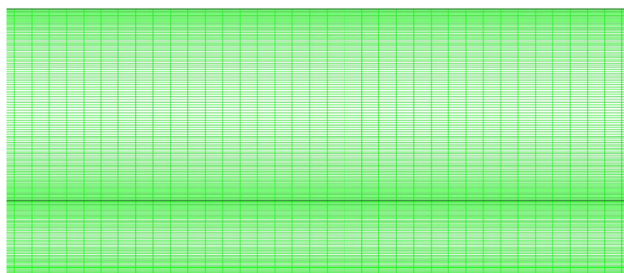


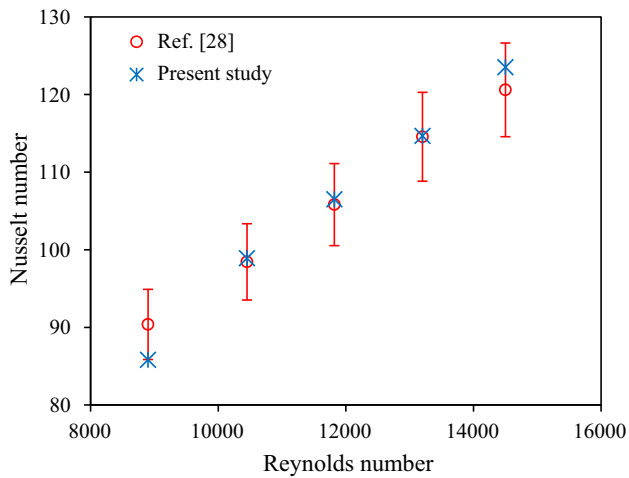
Fig. 3 Structured non-uniform grid for the computational domain

and Newtonian  $\text{Fe}_3\text{O}_4/\text{CNT}/\text{water}$  hybrid nanofluids will be reported by letters ‘NN’ and ‘N’, respectively.

Figure 5 illustrates the variations of viscosity ratio ( $\mu_{\text{nf,NN}}/\mu_{\text{nf,N}}$ ) for  $\phi_M = 0.7\%$  and  $\phi_{\text{CNT}} = 0.7\%$  at three different cross sections (i.e.,  $x = 0.1$  m,  $x = 0.5$  m, and  $x = 0.9$  m). For  $Re_{\text{nf}} = 500$ , by increasing the distance from the tube axis, viscosity of the non-Newtonian hybrid nanofluid diminishes severely at first, and then, its descending trend continues at a milder slope, and degree of variations increases with the increase in distance from the tube inlet. Near the tube axis, due to small values of shear rate and temperature, viscosity is high. However, by moving away from the tube axis toward the tube wall, both shear rate and temperature increase and consequently viscosity reduces. The results for  $Re_{\text{nf}} = 2000$  indicate that by moving away from the central regions of tube toward the tube wall, viscosity reduces and degree of viscosity variation is lower than that for  $Re_{\text{nf}} = 500$ . By increasing the Reynolds number at a fixed concentration, the thickness of velocity boundary layer reduces, and therefore, the velocity gradient increases. Therefore, there are two reasons for the negligible changes of viscosity in central regions of tube at cross section  $x = 0.1$  m. The first reason is that the shear rate is greater than  $60 \text{ s}^{-1}$  at most of points of this section, and consequently, fluid viscosity is constant. The second reason is that the thickness of thermal boundary layer in this area is small, which causes constant temperature of the hybrid nanofluid in central regions of tube, and thus, viscosity remains unchanged. By moving away from the tube inlet, the thermal boundary layer grows which augments the temperature of the nanofluid in vicinity of the tube wall and thus reduces the viscosity. Therefore, the velocity of nanofluid diminishes near the tube wall and increases at the tube axis, i.e., the velocity profile becomes flatter. As a result, the amount of shear rate increases near the tube wall and diminishes near the tube axis, which causes viscosity to diminish near the tube wall and increase near the tube axis. Therefore, it can be said that by moving away from the tube axis, viscosity of the non-Newtonian hybrid nanofluid near the tube wall diminishes; however, its behavior near the tube axis depends on whether the effect of viscosity reduction due to the rise of temperature is greater or the effect of viscosity increases due to the reduction of velocity gradient. Therefore, it is concluded that the effect of temperature increase overcomes the effect of temperature gradient reduction, and viscosity of the non-Newtonian nanofluid diminishes by moving away from the tube inlet. Furthermore, Fig. 5a, b shows that viscosity of the non-Newtonian nanofluid diminishes with the increase in Reynolds number. This can be justified based on the reduction of the velocity boundary layer thickness with increasing Reynolds number, which leads to the increase in

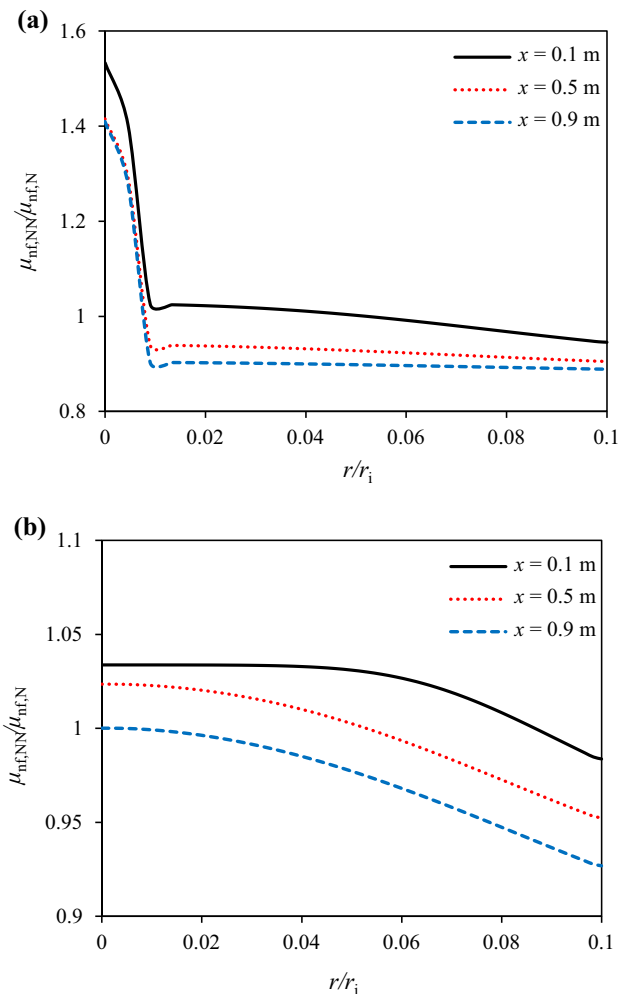
**Table 2** Grid independence study for non-Newtonian Fe<sub>3</sub>O<sub>4</sub>/CNT/water hybrid nanofluid at  $\varphi_M = 0.9\%$ ,  $\varphi_{CNT} = 1.35\%$ , and  $Re_{nf} = 2000$ 

Grid	$\dot{Q}/W$	Percentage difference	$\Delta p/Pa$	Percentage difference
800 × 25 × 25	33.92		120.1	
900 × 30 × 30	35.82	5.6	125.5	4.5
950 × 30 × 30	37.06	3.5	129.1	2.9
1000 × 30 × 30	37.92	2.3	132.1	2.3
<b>1000 × 35 × 35</b>	<b>38.23</b>	<b>0.8</b>	<b>133.7</b>	<b>1.2</b>
1100 × 35 × 35	38.51	0.7	134.6	0.67

**Fig. 4** Comparison between results obtained from the present study and experimental results of Ref. [28]

velocity gradient and thus the reduction of fluid viscosity. In addition, the comparison between the viscosities of the Newtonian and non-Newtonian hybrid nanofluids indicates that in central regions of the tube, viscosity of the non-Newtonian nanofluid is greater than that of the Newtonian nanofluid; however, in vicinity of the tube wall, the Newtonian fluid has a higher viscosity and by moving away from the tube inlet, the region in which viscosity of the Newtonian nanofluid is greater becomes vaster, since the viscosity of the non-Newtonian nanofluid diminishes by moving away from the tube wall. Both the temperature and shear rate are higher near the tube wall than the tube axis. Therefore, both of these factors lead to the viscosity reduction of the non-Newtonian nanofluids, while the opposite is true near the tube axis.

Figure 6 displays the variations of thermal conductivity ratio ( $k_{nf,NN}/k_{nf,N}$ ) for  $\varphi_M = 0.7\%$  and  $\varphi_{CNT} = 0.7\%$  at three different cross sections (i.e.,  $x = 0.1$  m,  $x = 0.5$  m, and  $x = 0.9$  m). For  $Re_{nf} = 500$ , by moving away from the tube axis toward the tube wall, thermal conductivity of the non-Newtonian nanofluid increases continually due to the higher temperature of nanofluid near the wall. The improvement of thermal conductivity with the increase in distance from the tube inlet is due to the higher nanofluid temperature resulting from the increase in heat transfer to

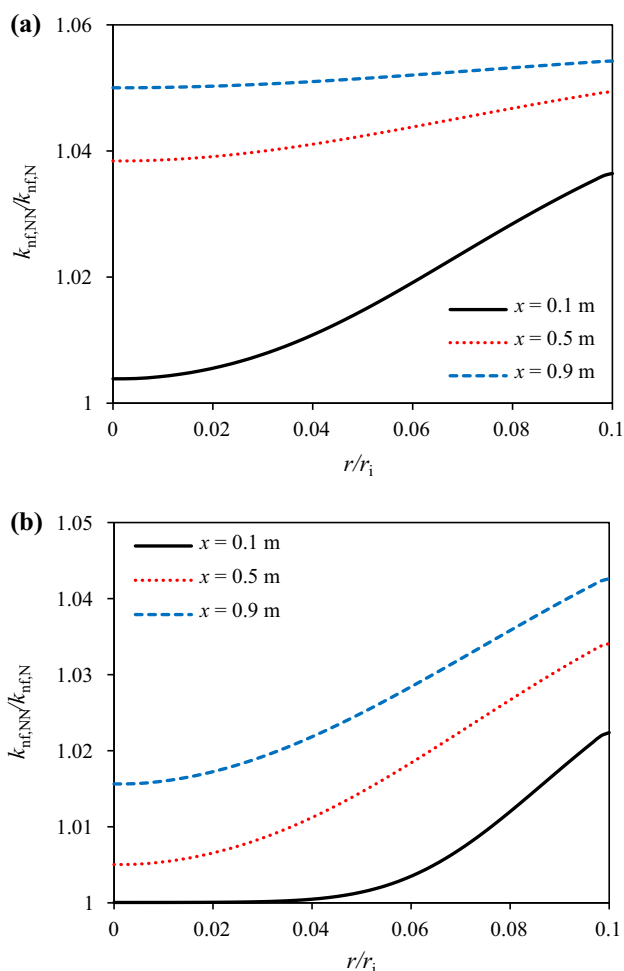
**Fig. 5** Viscosity ratio for  $\varphi_M = 0.7\%$  and  $\varphi_{CNT} = 0.7\%$  at three different cross sections for **a**  $Re_{nf} = 500$  and **b**  $Re_{nf} = 2000$ 

the nanofluid. Similar observations exist for  $Re_{nf} = 2000$ , with the difference that the slope of thermal conductivity increment near the tube wall is greater for  $Re_{nf} = 2000$ . This is due to the rise of nanofluid temperature near the tube wall, resulting from the lower thermal boundary layer thickness that occurs because of the flow velocity enhancement. Moreover, the comparison between thermal conductivity of the Newtonian and non-Newtonian nanofluids shows that thermal conductivity of the non-

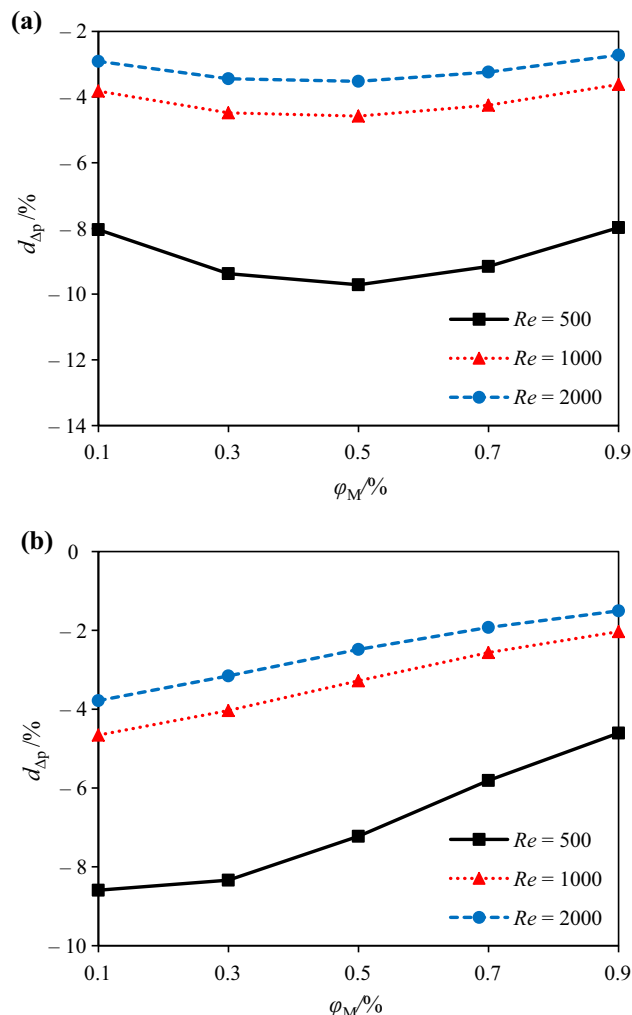
Newtonian nanofluid is always greater than that of the Newtonian nanofluid; however, the difference between thermal conductivities of the nanofluids reduces with the increase in Reynolds number. Considering the facts that the inlet temperature of nanofluid is 25 °C, and the thermal conductivity improves with the rise of temperature, it was predictable for the thermal conductivity of non-Newtonian nanofluid to always surpass that for the Newtonian nanofluid. In addition, increasing the Reynolds number reduces the thermal boundary layer thickness, and consequently, the internal layers of nanofluid are affected more slowly by wall temperature. This reduces the nanofluid temperature and thereby reduces the thermal conductivity of non-Newtonian nanofluid.

Figure 7 demonstrates the difference between the pressure drop of the Newtonian and non-Newtonian Fe<sub>3</sub>O<sub>4</sub>/CNT/water hybrid nanofluids ( $d_{\Delta p} = \frac{(\Delta p)_{NN} - (\Delta p)_N}{(\Delta p)_N} \times 100$ ) in terms of magnetite concentration at different Reynolds numbers. It is seen that the pressure drop of the non-

Newtonian nanofluid is always less than that of the Newtonian nanofluid. The minimum pressure drop difference (1.5%) is obtained at  $\varphi_M = 0.9\%$ ,  $\varphi_{CNT} = 1.35\%$ , and  $Re_{nf} = 2000$ , while the maximum difference (9.71%) occurs at  $\varphi_M = 0.5\%$ ,  $\varphi_{CNT} = 0.1\%$ , and  $Re_{nf} = 500$ . Additionally, it is observed that the difference between the pressure drop of the Newtonian and non-Newtonian nanofluids reduces with the increase in Reynolds number. According to Fig. 5, this is caused by the reduction in the difference between the average viscosity of the Newtonian and non-Newtonian nanofluids by increasing the Reynolds number. Furthermore, at  $\varphi_{CNT} = 0.1\%$ , the pressure drop difference augments when the magnetite concentration increases from 0.1 to 0.3% and then reduces by the further increment of magnetite concentration, while for  $\varphi_{CNT} = 1.35\%$ , the increase in magnetite concentration results in the reduction in the pressure drop difference. Besides, at  $\varphi_M = 0.1\%$ , the pressure drop difference rises



**Fig. 6** Thermal conductivity ratio for  $\varphi_M = 0.7\%$  and  $\varphi_{CNT} = 0.7\%$  at three different cross sections for **a**  $Re_{nf} = 500$  and **b**  $Re_{nf} = 2000$



**Fig. 7** Pressure drop at different Reynolds numbers in terms of magnetite concentration at **a**  $\varphi_{CNT} = 0.1\%$  and **b**  $\varphi_{CNT} = 1.35\%$



with increasing CNT concentration from 0.1 to 1.35%, while the opposite is true at higher magnetite concentrations. According to Eq. (22) and by considering the fact that the non-Newtonian and Newtonian nanofluids have the same density and friction factor at an identical Reynolds number, the difference between the pressure drop of the Newtonian and non-Newtonian nanofluids is only due to the difference between their viscosities. It can be concluded from the presented results that the assumption of constant thermal conductivity and viscosity of the hybrid nanofluid, at a low Reynolds number, leads to large errors in the computation of pressure drop; however, the obtained error decreases with the increase in Reynolds number.

The effects of magnetite concentration on the difference between the heat transfer rate of the Newtonian and non-Newtonian Fe<sub>3</sub>O<sub>4</sub>/CNT/water hybrid nanofluids ( $d_Q = \frac{\dot{Q}_{NN} - \dot{Q}_N}{\dot{Q}_N} \times 100$ ) at different Reynolds numbers are illustrated in Fig. 8. It is seen that the heat transfer rate of the non-Newtonian hybrid nanofluid is greater than that of the Newtonian nanofluid. The minimum difference (0.31%) is achieved at  $\varphi_M = 0.9\%$ ,  $\varphi_{CNT} = 1.35\%$ , and  $Re_{nf} = 500$ , while the maximum difference (1.23%) occurs at  $\varphi_M = 0.1\%$ ,  $\varphi_{CNT} = 1.35\%$ , and  $Re_{nf} = 1000$ . Additionally, it is observed that with the increase in Reynolds number, the difference between the heat transfer rate of the non-Newtonian and Newtonian nanofluids increases first and then decreases. Increasing the Reynolds number reduces the thermal conductivity and the thermal boundary layer thickness of the non-Newtonian nanofluid, which, respectively, reduces and increases the rate of heat transfer. In view of Fig. 8, it can be realized that at  $Re_{nf} = 1000$ , the effect of reducing the thickness of thermal boundary layer is dominant in comparison with the reduction of thermal conductivity, and therefore, the difference between the heat transfer rate of the Newtonian and non-Newtonian nanofluids increases. Meanwhile, for  $Re_{nf} = 2000$ , the reduction of thermal conductivity is dominant, which causes a decrease in the difference between the heat transfer rate of the non-Newtonian and Newtonian nanofluids. Moreover, Fig. 8 reveals that at magnetite concentrations of 0.1% and 0.3%, increasing the CNT concentration from 0.1 to 1.35% leads to an increase in the difference between the heat transfer rate of the Newtonian and non-Newtonian nanofluids, whereas the opposite is true for higher magnetite concentrations. Increasing the magnetite concentration leads to the increase in thermal conductivity of the non-Newtonian nanofluid and therefore the increase in nanofluid outlet temperature, and eventually to the increase in difference between the heat transfer rate of the non-Newtonian and Newtonian nanofluids. Further increasing the magnetite concentration leads to the decrease in the difference between the thermal conductivity

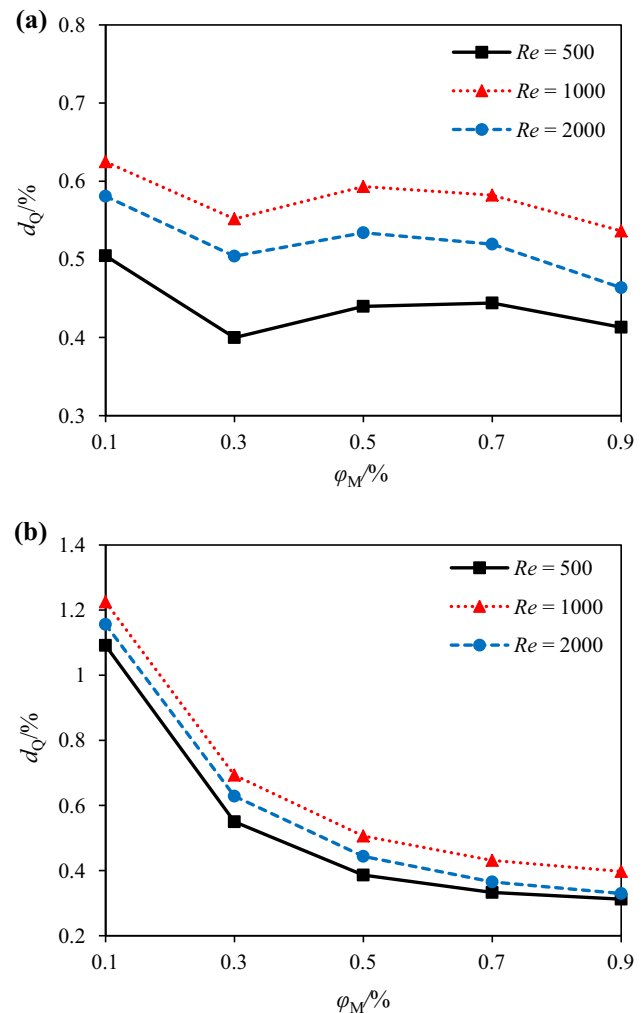


**Fig. 8** Heat transfer rate at different Reynolds numbers in terms of magnetite concentration at **a**  $\varphi_{CNT} = 0.1\%$  and **b**  $\varphi_{CNT} = 1.35\%$

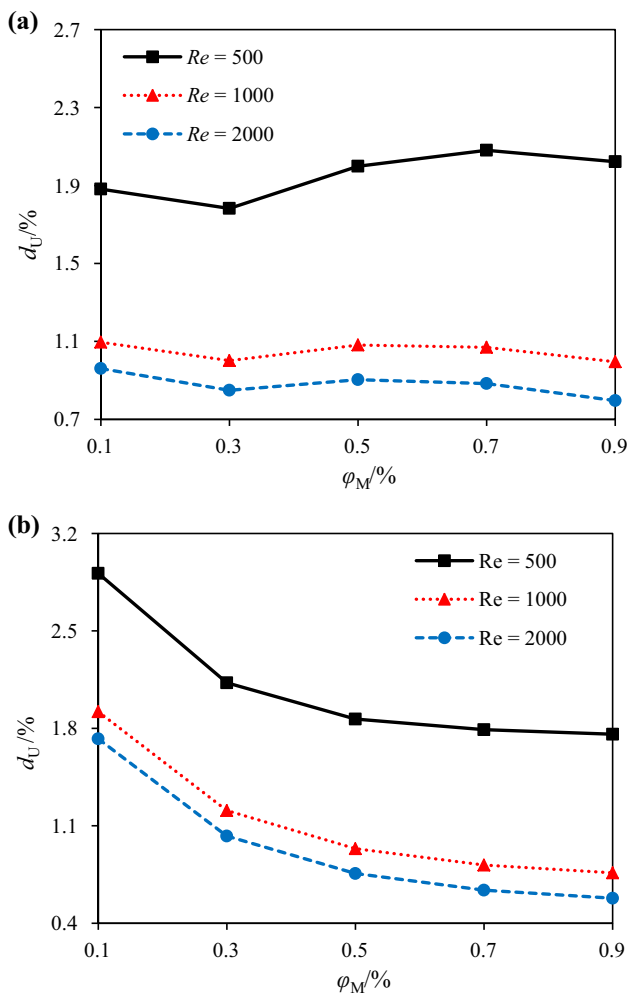
of the non-Newtonian and Newtonian nanofluids and therefore the decrease in the heat transfer rate difference. The results also show that there is no specific pattern on the relationship between the difference in the heat transfer rate of the Newtonian and non-Newtonian nanofluids and the magnetite concentration.

Figure 9 shows the difference between the overall heat transfer coefficient of the Newtonian and non-Newtonian Fe<sub>3</sub>O<sub>4</sub>/CNT/water hybrid nanofluids ( $d_U = \frac{U_{NN} - U_N}{U_N} \times 100$ ) in terms of magnetite concentration at various Reynolds numbers. It is clear that the overall heat transfer coefficient of the non-Newtonian hybrid nanofluid is greater than that of the Newtonian nanofluid. The minimum difference of the overall heat transfer coefficients (0.58%) is obtained at  $\varphi_M = 0.9\%$ ,  $\varphi_{CNT} = 1.35\%$ , and  $Re_{nf} = 2000$ , while the maximum difference (2.91%) is achieved at  $\varphi_M = 0.1\%$ ,  $\varphi_{CNT} = 1.35\%$ , and  $Re = 500$ . Furthermore, the results depicted that the variations of difference between the

overall heat transfer coefficient of the Newtonian and non-Newtonian nanofluids with the magnetite and CNT concentrations are similar to that of the difference between the heat transfer rates of these nanofluids. According to the results presented in Fig. 9, it can be concluded that the difference between the overall heat transfer coefficient of the Newtonian and non-Newtonian nanofluids is less than 3%, which is not significant.

The impacts of magnetite concentration on the difference between the effectiveness of the heat exchangers containing Newtonian and non-Newtonian Fe<sub>3</sub>O<sub>4</sub>/CNT/water hybrid nanofluids ( $d_e = \frac{\epsilon_{NN} - \epsilon_N}{\epsilon_N} \times 100$ ) at different Reynolds numbers are illustrated in Fig. 10. In view of Eq. (16), it can be realized that the trend of effectiveness variations is similar to that of the heat transfer rate variations. Therefore, all the conclusions reached above regarding the heat transfer rate are also true for the effectiveness.

The pumping power indicates the amount of energy utilized in a heat exchanger. Figure 11 depicts the difference between the pumping powers of the Newtonian and non-Newtonian Fe<sub>3</sub>O<sub>4</sub>/CNT/water hybrid nanofluids ( $d_U = \frac{U_{NN} - U_N}{U_N} \times 100$ ) in terms of magnetite concentration at different Reynolds numbers. It is seen that at a constant Reynolds number, the non-Newtonian hybrid nanofluid always requires less pumping power than the Newtonian nanofluid. The minimum pumping power difference (1.5%) is obtained at  $\phi_M = 0.9\%$ ,  $\phi_{CNT} = 1.35\%$ , and  $Re_{nf} = 2000$ , while the maximum difference (9.71%) occurs at  $\phi_M = 0.5\%$ ,  $\phi_{CNT} = 0.1\%$ , and  $Re_{nf} = 500$ . In view of Eq. (21), and considering the same average velocity for the Newtonian and non-Newtonian nanofluids at similar Reynolds numbers, the difference between the pumping power of the Newtonian and non-Newtonian nanofluids is only related to the difference between their pressure drops. Therefore, at a low Reynolds number, the



**Fig. 9** Overall heat transfer coefficient at different Reynolds numbers in terms of magnetite concentration at **a**  $\phi_{CNT} = 0.1\%$  and **b**  $\phi_{CNT} = 1.35\%$

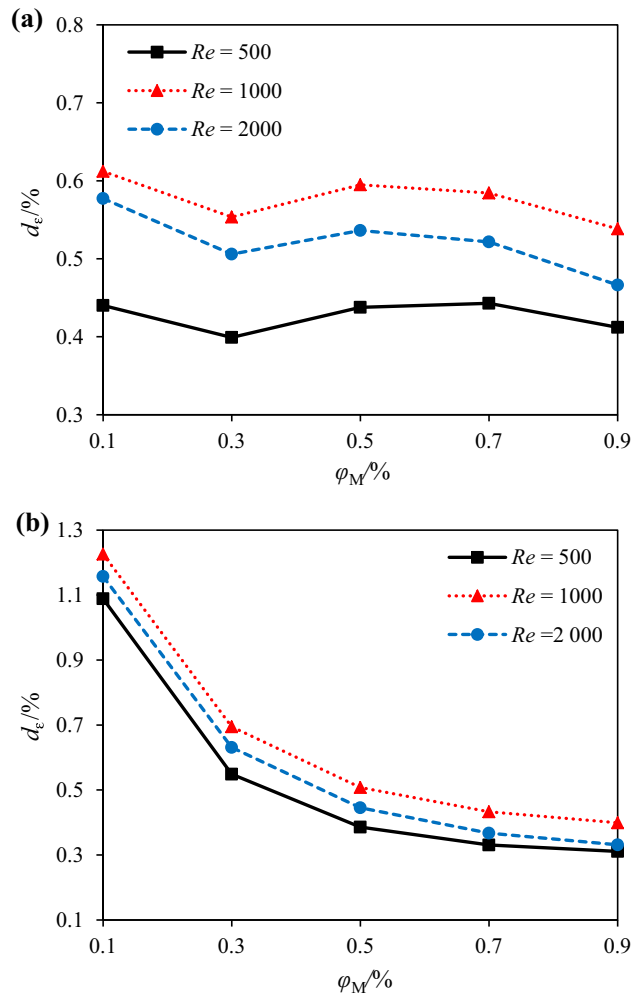


**Fig. 10** Effectiveness of heat exchanger at different Reynolds numbers in terms of magnetite concentration at **a**  $\phi_{CNT} = 0.1\%$  and **b**  $\phi_{CNT} = 1.35\%$

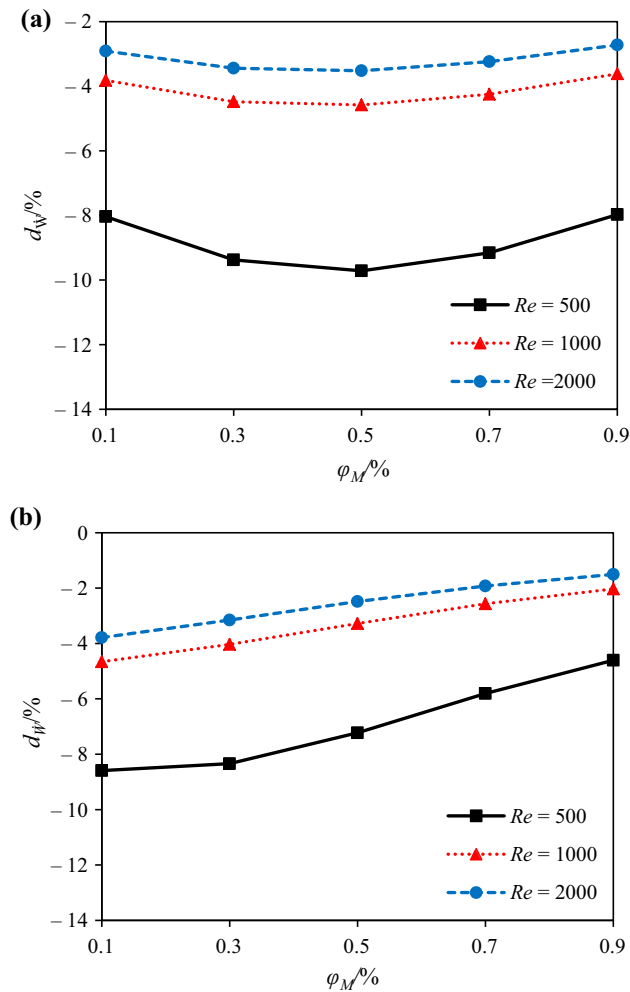


**Fig. 11** Pumping power of heat exchanger at different Reynolds numbers in terms of magnetite concentration at **a**  $\phi_{CNT} = 0.1\%$  and **b**  $\phi_{CNT} = 1.35\%$

assumption of constant properties leads to a considerable increase in the pumping power of heat exchangers, whereas the difference reduces with increasing Reynolds number.

The influences of magnetite concentration on the difference between the  $PEC$  of the heat exchangers containing Newtonian and non-Newtonian Fe<sub>3</sub>O<sub>4</sub>/CNT/water hybrid nanofluids ( $d_{PEC} = \frac{PEC_{NN} - PEC_N}{PEC_N} \times 100$ ) at different Reynolds numbers are displayed in Fig. 12. It is observed that the heat exchanger containing Newtonian nanofluid has a higher  $PEC$  than that containing non-Newtonian nanofluid. The minimum difference (18.24%) is obtained at  $\phi_M = 0.1\%$ ,  $\phi_{CNT} = 1.35\%$ , and  $Re_{nf} = 500$ , while the maximum difference (19.60%) is achieved at  $\phi_M = 0.9\%$ ,  $\phi_{CNT} = 1.35\%$ , and  $Re_{nf} = 2000$ . Moreover, it is seen that the difference between the  $PEC$  of the heat exchangers containing Newtonian and non-Newtonian nanofluids increases with the increase in Reynolds number. In addition, at  $\phi_{CNT} = 0.1\%$ , the  $PEC$  difference reduces when the

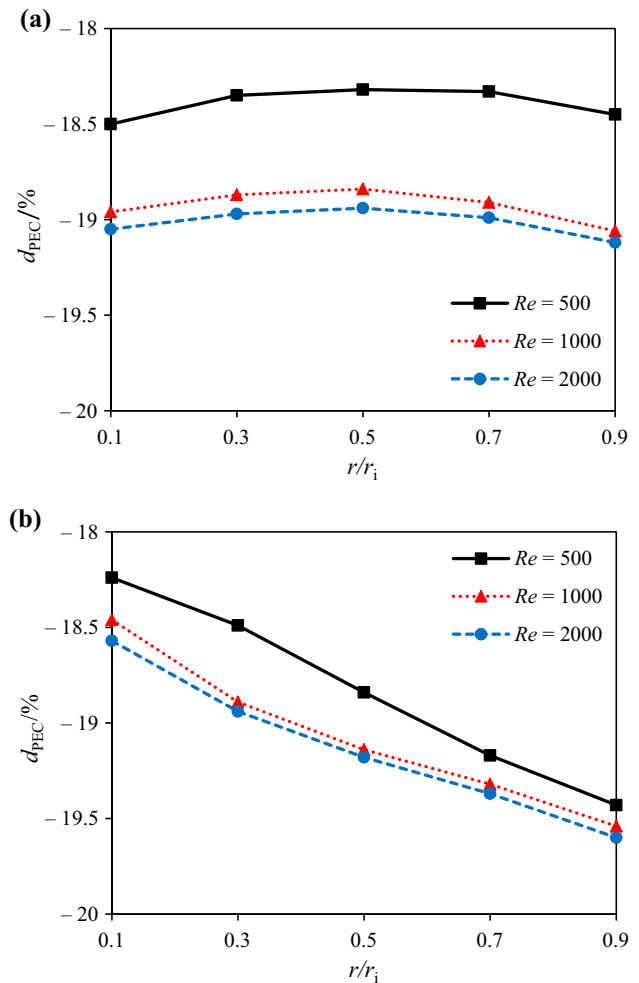


**Fig. 12** Performance evaluation criterion of heat exchanger at different Reynolds numbers in terms of magnetite concentration at **a**  $\phi_{CNT} = 0.1\%$  and **b**  $\phi_{CNT} = 1.35\%$

magnetite concentration rises from 0.1 to 0.5% and then augments by the further increment of magnetite concentration, while for  $\phi_{CNT} = 1.35\%$ , the increase in magnetite concentration results in the increase in the  $PEC$  difference. Moreover, at  $\phi_M = 0.1\%$ , the  $PEC$  difference reduces with the increase in CNT concentration from 0.1 to 1.35%, while the opposite is happened at higher magnetite concentrations. It can be said that the assumption of constant properties of the Fe<sub>3</sub>O<sub>4</sub>/CNT/water hybrid nanofluid leads to large errors in the computation of  $PEC$ .

Finally, in order for the readers to be able to reproduce the results and to make clear comparisons, the heat transfer rate, pumping power, friction factor, and Nusselt number of Newtonian and non-Newtonian nanofluids at  $Re_{nf} = 2000$  are tabulated in Table 3.

**Table 3** Hydrothermal aspects of the studied double-pipe heat exchanger filled with Newtonian and non-Newtonian Fe<sub>3</sub>O<sub>4</sub>/CNT/water hybrid nanofluids

$\varphi_M/\%$	$\varphi_{CNT}/\%$	$\dot{Q}_{NN}/W$	$\dot{Q}_N/W$	$\dot{W}_{NN}/W$	$\dot{W}_N/W$	$f_{NN}$	$f_N$	$Nu_{NN}$	$Nu_N$
0.1	0.1	35.99	35.78232	0.000136	0.00014	0.000021	0.000022	3.478	6.894
0.3	0.1	36.40	36.21853	0.000153	0.000159	0.000024	0.000025	3.455	6.851
0.5	0.1	36.57	36.37479	0.000175	0.000181	0.000028	0.000029	3.446	6.830
0.7	0.1	36.81	36.61522	0.000198	0.000205	0.000032	0.000033	3.433	6.689
0.9	0.1	37.19	37.01716	0.000221	0.000227	0.000037	0.000038	3.413	6.770
0.1	1.35	29.49	29.14805	0.000179	0.000186	0.000029	0.000030	3.805	7.479
0.3	1.35	34.48	34.26205	0.000203	0.00021	0.000033	0.000034	3.523	6.973
0.5	1.35	36.84	36.68143	0.000225	0.00023	0.000037	0.000038	3.418	6.782
0.7	1.35	37.88	37.74574	0.000242	0.000247	0.000041	0.000041	3.375	6.705
0.9	1.35	38.23	38.10522	0.000254	0.000258	0.000043	0.000044	3.359	6.678

## Conclusions

In this research, the hydrothermal performance of the non-Newtonian Fe<sub>3</sub>O<sub>4</sub>/CNT/water hybrid nanofluid considering temperature-dependent thermal conductivity and viscosity is numerically evaluated in a double-pipe mini-channel heat exchanger compared with the Newtonian Fe<sub>3</sub>O<sub>4</sub>/CNT/water nanofluid with constant thermal conductivity and viscosity. The comparison is used in order to find how the assumption of constant thermophysical properties of a hybrid nanofluid affects the hydrothermal characteristics in a double-pipe heat exchanger. The obtained results show that in central region of the tube, the non-Newtonian hybrid nanofluid has a higher viscosity compared to the Newtonian nanofluid, while the opposite is true in vicinity of the tube wall. Besides, it is found that the non-Newtonian hybrid nanofluid always has a higher thermal conductivity than the Newtonian nanofluid. In addition, it is seen that the heat transfer rate, overall heat transfer coefficient, and effectiveness of the non-Newtonian hybrid nanofluid are greater than those of the Newtonian hybrid nanofluid, while the opposite is true for the pressure drop, pumping power, and performance evaluation criterion. The difference between the heat transfer rate, overall heat transfer coefficient, effectiveness, and performance evaluation criterion of Newtonian and non-Newtonian hybrid nanofluids augments with the increase in Reynolds number, whereas the difference between the pressure drop and pumping power of nanofluids reduces with increasing Reynolds number. Furthermore, increase in magnetite and CNT concentrations has no particular effect on the considered parameters. Finally, it can be concluded that by supposing that the Fe<sub>3</sub>O<sub>4</sub>/CNT/water hybrid nanofluid is a Newtonian fluid with constant thermal conductivity and viscosity, large errors occur in the computation of pressure drop (1.5–9.71%), pumping power (1.5–9.71%), and performance evaluation criterion (18.24–19.60%), whereas the errors in the computation of heat transfer rate (0.31–1.23%), overall heat transfer coefficient (0.58–2.91%), and effectiveness (0.31–1.23%) are not

considerable. The results of this study could provide guidelines to better understand the real behaviors of hybrid nanofluids in heat exchangers.

## References

1. Omidi M, Farhadi M, Jafari M. A comprehensive review on double pipe heat exchangers. *Appl Therm Eng.* 2017;110:1075–90.
2. Rashidi S, Eskandarian M, Mahian O, Poncet S. Combination of nanofluid and inserts for heat transfer enhancement. *J Therm Anal Calorim.* 2018:1–24.
3. Esfahani NN, Toghraie D, Afrand M. A new correlation for predicting the thermal conductivity of ZnO–Ag (50%–50%)/water hybrid nanofluid: an experimental study. *Powder Technol.* 2018;323:367–73.
4. Choi S, Estman J. Enhancing thermal conductivity of fluids with nanoparticles. *ASME-Publications-Fed.* 1995;231:99–106.
5. Rezaei O, Akbari OA, Marzban A, Toghraie D, Pourfatah F, Mashayekhi R. The numerical investigation of heat transfer and pressure drop of turbulent flow in a triangular microchannel. *Physica E.* 2017;93:179–89.
6. Maddah H, Alizadeh M, Ghasemi N, Alwi SRW. Experimental study of Al<sub>2</sub>O<sub>3</sub>/water nanofluid turbulent heat transfer enhancement in the horizontal double pipes fitted with modified twisted tapes. *Int J Heat Mass Transf.* 2014;78:1042–54.
7. Mousavi SV, Sheikholeslami M, Gerdroodbary MB. The Influence of magnetic field on heat transfer of magnetic nanofluid in a sinusoidal double pipe heat exchanger. *Chem Eng Res Des.* 2016;113:112–24.
8. Saeedan M, Nazar ARS, Abbasi Y, Karimi R. CFD Investigation and neural network modeling of heat transfer and pressure drop of nanofluids in double pipe helically baffled heat exchanger with a 3-D fined tube. *Appl Therm Eng.* 2016;100:721–9.
9. Sarafraz M, Hormozi F, Nikkhal V. Thermal performance of a counter-current double pipe heat exchanger working with COOH-CNT/water nanofluids. *Exp Therm Fluid Sci.* 2016;78:41–9.
10. Kumar NR, Bhramara P, Sundar LS, Singh MK, Sousa AC. Heat transfer, friction factor and effectiveness of Fe<sub>3</sub>O<sub>4</sub> nanofluid flow in an inner tube of double pipe U-bend heat exchanger with and without longitudinal strip inserts. *Exp Therm Fluid Sci.* 2017;85:331–43.
11. Hussein AM. Thermal performance and thermal properties of hybrid nanofluid laminar flow in a double pipe heat exchanger. *Exp Therm Fluid Sci.* 2017;88:37–45.

12. Shirvan KM, Mamourian M, Mirzakhani S, Ellahi R. Numerical investigation of heat exchanger effectiveness in a double pipe heat exchanger filled with nanofluid: a sensitivity analysis by response surface methodology. *Powder Technol.* 2017;313:99–111.
13. Esfe MH, Esfandeh S, Afrand M, Rejvani M, Rostamian SH. Experimental evaluation, new correlation proposing and ANN modeling of thermal properties of EG based hybrid nanofluid containing ZnO-DWCNT nanoparticles for internal combustion engines applications. *Appl Therm Eng.* 2018;133:452–63.
14. Shahsavari A, Saghafian M, Salimpour M, Shafii M. Effect of temperature and concentration on thermal conductivity and viscosity of ferrofluid loaded with carbon nanotubes. *Heat Mass Transf.* 2016;52:2293–301.
15. Theres Baby T, Sundara R. Surfactant free magnetic nanofluids based on core-shell type nanoparticle decorated multiwalled carbon nanotubes. *J Appl Phys.* 2011;110:064325.
16. Felicia LJ, Philip J. Magnetorheological properties of a magnetic nanofluid with dispersed carbon nanotubes. *Phys Rev E.* 2014;89:022310.
17. Sundar LS, Singh MK, Sousa AC. Enhanced heat transfer and friction factor of MWCNT–Fe<sub>3</sub>O<sub>4</sub>/water hybrid nanofluids. *Int Commun Heat Mass Transf.* 2014;52:73–83.
18. Shahsavari A, Saghafian M, Salimpour M, Shafii M. Experimental investigation on laminar forced convective heat transfer of ferrofluid loaded with carbon nanotubes under constant and alternating magnetic fields. *Exp Therm Fluid Sci.* 2016;76:1–11.
19. Harandi SS, Karimipour A, Afrand M, Akbari M, D’Orazio A. An experimental study on thermal conductivity of F-MWCNTs–Fe<sub>3</sub>O<sub>4</sub>/EG hybrid nanofluid: effects of temperature and concentration. *Int Commun Heat Mass Transf.* 2016;76:171–7.
20. Hemmat Esfe M, Hassani Ahangar MR, Toghraie D, Hajmohammad MH, Rostamian H, Tourang H. Designing artificial neural network on thermal conductivity of Al<sub>2</sub>O<sub>3</sub>–water–EG (60–40%) nanofluid using experimental data. *J Therm Anal Calorim.* 2016;126:837–43.
21. Sandeep N, Malvandi A. Enhanced heat transfer in liquid thin film flow of non-Newtonian nanofluids embedded with graphene nanoparticles. *Adv Powder Technol.* 2016;27:2448–56.
22. Shahsavari A, Salimpour MR, Saghafian M, Shafii MB. Effect of magnetic field on thermal conductivity and viscosity of a magnetic nanofluid loaded with carbon nanotubes. *J Mech Sci Technol.* 2016;30:809–15.
23. Berger P, Adelman NB, Beckman KJ, Campbell DJ, Ellis AB, Lisensky GC. Preparation and properties of an aqueous ferrofluid. *J Chem Educ.* 1999;76:943.
24. Shahsavari A, Bahiraei M. Experimental investigation and modeling of thermal conductivity and viscosity for non-Newtonian hybrid nanofluid containing coated CNT/Fe<sub>3</sub>O<sub>4</sub> nanoparticles. *Powder Technol.* 2017;318:441–50.
25. Bahiraei M, Berahmand M, Shahsavari A. Irreversibility analysis for flow of a non-Newtonian hybrid nanofluid containing coated CNT/Fe<sub>3</sub>O<sub>4</sub> nanoparticles in a minichannel heat exchanger. *Appl Therm Eng.* 2017;125:1083–93.
26. Bahiraei M, Godini A, Shahsavari A. Thermal and hydraulic characteristics of a minichannel heat exchanger operated with a non-Newtonian hybrid nanofluid. *J Taiwan Inst Chem Eng.* 2018;84:149–61.
27. Heydari M, Toghraie D, Akbari OA. The effect of semi-attached and offset mid-truncated ribs and Water/TiO<sub>2</sub> nanofluid on flow and heat transfer properties in a triangular microchannel. *Therm Sci Eng Prog.* 2017;2:140–50.
28. Duangthongsuk W, Wongwises S. An experimental study on the heat transfer performance and pressure drop of TiO<sub>2</sub>-water nanofluids flowing under a turbulent flow regime. *Int J Heat Mass Transf.* 2010;53:334–44.

**Publisher's Note** Springer Nature remains neutral with regard to jurisdictional claims in published maps and institutional affiliations.